VCE EARLY ACOUSTIC TEST RESULTS OF GENERAL ELECTRIC'S HIGH-RADIUS RATIO COANNULAR PLUG NOZZLE+

Paul R. Knott, J.F. Brausch, P.K. Bhutiani,
R.K. Majjigi, V.L. Doyle
General Electric Co., Cincinnati, Ohio

SUMMARY

Results of NASA Lewis Research Center/General Electric Company Variable Cycle Engine (VCE) early acoustic engine and model scale tests are presented. A summary of an extensive series of far-field acoustic, advanced acoustic, and exhaust plume velocity measurements with a laser velocimeter of inverted velocity and temperature profile, high-radius-ratio coannular plug nozzles on a YJ101 VCE static engine test vehicle are reviewed. Select model scale simulated flight acoustic measurements for an unsuppressed and a mechanical suppressed coannular plug nozzle are also discussed. The engine acoustic nozzle tests verify previous model scale noise reduction measurements. The engine measurements show 4-6 PNdB aft quadrant jet noise reduction and up to 7 PNdB forward quadrant shock noise reduction relative to a fully mixed conical nozzle at the same specific thrust and mixed pressure ratio. The influences of outer nozzle radius ratio, inner stream velocity ratio, and area ratio are discussed. Also, laser velocimeter measurements of mean velocity and turbulent velocity of the YJ101 engine are illustrated. Select model scale static and simulated flight acoustic measurements are shown which corroborate that coannular suppression is maintained in forward speed. In addition, the outlook for achieving jet noise abatement levels for high performance supersonic aircraft on the order of current subsonic commercial vehicles is discussed.

INTRODUCTION

Over the past decade, government and industry have exerted considerable research and technology efforts toward developing understanding of jet noise generation, concepts for its reduction, and practical means for suppressor implementation. In particular, the General Electric Company, under NASA-Lewis sponsorship, has undertaken extensive model scale and engine acoustic test programs (References 1,2, and work done under contract by J. Vdoviak, P.R. Knott, et al., entitled "VCE Early Acoustic Test - Forward Variable Area By Pass Injector and Coannular Acoustic Nozzle Test," to be published in 1980) to quantify the static and flight acoustic and aerodynamic characteristics for inverted velocity and temperature profile coannular plug nozzles, unsuppressed and suppressed.

+ The work reported here was sponsored by the NASA Lewis Research Center under Contracts NAS3-20582 and NAS3-21608.

This paper reviews an extensive series of static engine acoustic tests using General Electric's variable cycle engine (VCE) features tested on a modified YJ101 engine propulsion system in October of 1978. These results show that for unsuppressed high-radius-ratio coannular plug nozzles, substantial static jet mixing and shock noise reduction is obtained in engine scale. The paper also shows that for simulated flight, this level of noise reduction is maintained. In addition, a projected outlook for achieving greater jet noise reduction for SCR vehicles on the order of current subsonic commerical aircraft is briefly discussed.

The authors express their appreciation to Al Powers, Jim Stone, Orlando Gutierrez, Howard Wesoky, and Jack Whitlow of NASA-Lewis Research Center for their high interest in the word accomplished, their probing questions, and their expectancy of technical excellence.

SYMBOLS

Values are given in SI units.

A_o	ambient speed of sound; m/sec
A_r^i	nozzle system area ratio (Inner stream nozzle area/Outer stream area); dimensionless
a	speed of sound; m/sec
c_j	speed of sound of core stream, m/sec
c_{sj}	speed of sound of the thermal acoustic shield, m/sec
EPNL	effective perceived noise level, EPNdB
F	ideal total thrust, newtons
F_i	freefield SPL, dB
F_{ref}	reference thrust, newtons
G_i	ground plane measured SPL, dB
i	index of one-third octave band
$\dot{m}_j^i$	ideal inner stream (or far stream) mass flow rate, grams/sec
$\dot{m}_j^o$	ideal outer stream (or core stream) mass flow rate, grams/sec

$\dot{m}_T$ ideal total mass flow rate $(\dot{m}_j^o + \dot{m}_j^i)$, grams/sec

Pi engine centerline measured SPL, dB

P_r^{eff} effective pressure ratio for coannular nozzles, dimensionless

P_r^i inner stream (or fan stream) nozzle pressure ratio, dimensionless

P_r^o outer stream (or core stream) nozzle pressure ratio, dimensionless

PNL perceived noise level, PNdB

PNLN normalized perceived noise level

re: $10 \log\left\{\frac{F}{Fref}\left(\frac{\rho_j^{mix}}{\rho_o}\right)^{\omega-1}\right\}$, PNdB

R_i ground plane microphone weighting factor (see table 1)

R_r^o outer stream radius ratio (defined as a ratio of the radius to the throat inner diameter to the radius to the throat outer diameter of the nozzle), dimensionless

S_i engine centerline microphone weighting factor (see table 1)

SPL sound pressure level, dB

u' laser velocimeter measured turbulence velocity (axial direction), m/sec

u_p laser velocimeter measured peak mean velocity, m/sec

$\bar{U}$ laser velocimeter mean velocity (axial direction), m/sec

V_j^i ideal inner stream (or fan stream) velocity, m/sec

V_j^o ideal outer stream (or core stream) velocity, m/sec

V_j^{mix} specific thrust (defined as a ratio of the ideal total thrust to the ideal total mass flow rate) $\frac{\dot{m}_j^o V_j^o + \dot{m}_j^i V_j^i}{\dot{m}_T}$, m/sec

V_{sj} velocity of the thermal acoustic shield, m/sec

V_r^i velocity ratio (V_j^i/V_j^o), dimensionless

$$\beta_j^{mix} \quad \left\{\left[\left(P_r^{eff}\right)^{\frac{\gamma-1}{\gamma}} - 1\right]\frac{2}{\gamma-1} - 1\right\}, \text{ dimensionless}$$

where

$$P_r^{eff} \equiv \frac{P_r^o + P_r^i A_r^i}{1 + A_r^i}; \quad \gamma = 1.4$$

TEST APPARATUS AND DATA REDUCTION PROCEDURES

The test results presented in this paper were obtained from two facilities: 1) General Electric's/Edwards Air Force Base Out Door Engine Test Facility, and 2) General Electric's Model Scale Anechoic Free-Jet Test Facility. Discussed below are brief descriptions of these facilities and the basic test arrangements and data reduction procedures used in processing the data.

General Electric/Edwards Air Force Base Out Door Engine Test Facility

For all the engine tests presented, the General Electric/Edwards Flight Test Center North Test Site was used. Figure 1 shows the general layout of the test site showing the concrete paved sound field. It has a 48.77 m (160 ft) forward quadrant radius and a 82.3 m (270 ft) aft quadrant radius with a 22.86 m (75 ft) lateral sideline connecting the two arcs. Figure 2 shows the YJ101 engine with a treated inlet for eliminating fan inlet radiated noise and a baseline conical nozzle. Figure 3 shows the inverted velocity and temperature high-radius-ratio coannular plug nozzle configuration. Figures 4 and 5 show the G.E. laser velocimeter system and a NASA Ames sideline traversing microphone systems used for diagnostic velocity profile and noise identification respectively.

A typical sound field microphone layout for the engine test results is illustrated in Figure 6. It consists of a 30.48 m (100 ft) radius microphone array at 10^o increments from 10^o to 160^o and a 21.34 m (70 ft) lateral sideline array with ground plane microphones located at $\theta_j = 35^o$, 115^o, 125^o, 135^o, 145^o, 150^o, 155^o, 160^o, and 165^o. For the 30.48 m (100 ft) radius arrangement, engine centerline height microphones and ground plane microphones were used as illustrated in Figure 7. For these measurements the farfield arc data gathered from the two-microphone system were corrected to free-field and merged using the following scheme:*

* The method selected for the two microphone merging was based on information provided by the Boeing Airplane Company in Seattle, Washington.

$$F_i = R_i\ (G_i-6) + S_i\ (P_i-3)$$

where

i = index of one-third octave band
F_i = freefield SPL
G_i = ground plane measured SPL
P_i = engine centerline measured SPL
R_i = ground plane microphone weighting factor (see Table 1)
S_i = engine centerline microphone weighting factor (see Table 1)

Figure 8 shows an illustration of this spectral merging technique for typical conical and coannular plug nozzle measurements.

General Electric Model Scale Anechoic Free-Jet Test Facility

For Model scale static and simulated flight acoustic test measurements, the General Electric Company has developed a large free-jet anechoic test facility (References 3,4, and 5). Figure 9 shows a schematic diagram of facility. The General Electric facility is one of the largest of its type in the United States. The chamber is 22 meters (72 ft) high and 13 meters (42 ft) in diameter. The anechoic characteristics are 220 Hz cut off frequency, 0.99 absorption coefficient for frequencies above 220 Hz, and the chamber ambient noise less than 40 dB. The air supply system permits scale model jet nozzles with an equivalent diameter of up to 152 millimeters (6 in.), for single or coannular jet nozzle configuration - statically and in simulated flight up to $V_{a/c} \simeq 122$ m (400 fps).

TEST RESULTS AND DISCUSSION

Under two NASA-Lewis sponsored small-scale model nozzle test programs (References 1,2, and 6), substantial jet and shock noise reduction (4-6 PNdB static) at good thrust coefficients ($C_{fg} = .974$ at a take-off Mach number of .36) has been observed. Described below are verifications of these test results for a YJ101 engine using a unique high-radius-ratio plug nozzle exhaust system designed for an inverted velocity profile. Other engine test results and simulated flight measurements from model scale free-jet tests are also covered.

Verification of Coannular Plug Nozzle Jet and Shock Noise Reduction

Figures 10 and 11 illustrate the YJ101 engine coannular plug nozzle jet and shock noise reductions presented on a typical product engine size of .9032 m^2 (1400 in^2) and at an acoustic range of 731.5 m (2400 ft) sideline. Figure 10 shows the measured peak PNL jet noise reduction relative to the conical nozzle baseline for all the engine test results. The ordinate is peak PNL normalized with respect to ideal total thrust and static jet density, while

the abscissa is the ideal specific thrust, defined as the ideal total thrust divided by the total weight flow. The results show that in the range of 488 m/sec (1600 fps) to 701 m/sec (2300 fps), an average of 4 to 6 PNdB coannular plug nozzle jet noise reduction is realized. In the lower specific thrust range (381 m/sec (1250 fps)), the engine coannular plug nozzle jet noise benefit is observed to diminish due to engine operation at off-optimum velocity ratio.

Figure 11 shows the PNL at $\theta_i = 50^o$ as a function of shock strength parameter, β_j^{mix}, for the engine tests. One notes an almost uniform 7 PNdB static shock noise reduction for the coannular plug nozzle over the conic nozzle in the range of interest (10 log β_j^{mix} = -3 to 0).

For an illustration of the typical field shape and spectral characteristics between the engine baseline conical nozzle and coannular plug nozzles, Figures 12 and 13 are presented. The results show that the inverted velocity profile coannular plug nozzle jet noise reduction is measured at all observation angles and over all frequency bands.

Influence of Coannular Plug Nozzle Geometry on Jet Noise Reduction

Two key coannular plug nozzle geometric parameters which influence the jet noise signature and which are important to the mechanical design engineer are the outer stream radius-ratio (R_r^o) and the inner stream to outer stream area (A_r^i). Engine tests included nozzles of R_r^o = .816, .853, and .875 at an A_r^i = .2, and A_r^i = .475, .2, .1, $\sim$0 at an R_r^o = .853. Figures 14 and 15 illustrate the results of these engine acoustic measurements.

Shown in Figure 14 are the results of the radius ratio study. These engine acoustic measurements show that at high specific thrust (533 m/sec(1749 fps) to .762 m/sec (2500 fps)), the reduction of PNL at the same specific thrust is due to increasing R_r^o. The results indicate that the coannular plug nozzle jet noise reduction is close to a 6th power law on radius ratio.

Figure 15 presents the engine test results for the area ratio study. In the specific thrust range of 381 m/sec (1250 fps) to 610 m/sec (2000fps), the trend observed is that as A_r^i decreases, so does the peak PNL jet noise. At the higher specific thrusts (610 m/sec (2000 fps) to 700 m/sec (2296 fps)), the A_r^i = .2 shows the lowest noise, the A_r^i = .1 about ½ PNdB higher, and the $A_r^i \sim 0$ about 1.5 PNdB higher than the A_r^i = .2 data. This would correspond to a $-1.39 * \log_{10}(1+A_r^i)$ dependency for peak angle jet noise at typical takeoff sideline engine cycle conditions.

ACOUSTIC SCALING RESULTS

To illustrate acoustic scaling of typical model scale test measurements taken in General Electric's anechoic free-jet and compared with the YJ101 engine measurements for a conical nozzle and coannular plug nozzle, the following results are shown. Figures 16 and 17 show comparisons of normalized peak PNL from model and YJ101 engine tests for a conical and coannular plug nozzles (R_r^o = .853 and A_r^i = .2). All data have been scaled to typical product engine size and acoustic range. Excellent agreement is observed for both the configurations. Figures 18 and 19 show engine and model test comparisons for a coannular plug nozzle at a specific thrust of approximately 594 m/sec (1950 fps). Figure 18 compares PNL directivity whereas Figure 19 compares spectra at θ_i=50°, 90°, 130°. Again good scaling is observed.

THEORY DATA COMPARISONS AND EPNL PROJECTIONS

Theory Data Comparisons

Under NAS3-20619, a unique coannular jet and shock noise prediction method was developed (Reference 8). The prediction procedure developed was evolved from a modern theoretical acoustic point-of-view using experimentally determined information from model tests for a universal source spectrum at θ_i=90° and fluid acoustic shielding function. Figures 20 through 22 illustrate the theory/engine data comparisons for a coannular plug nozzle.

Shown in Figure 20 are engine acoustic measurements compared with predictions of OASPL for three engine conditions (typical of takeoff sideline, cut-back and approach conditions). The data/theory comparisons are at actual YJ101 engine size. Spectral data/theory comparisons for the take-off sideline condition and the cut-back condition are shown in Figure 21 and 22, respectively. The comparisons between theory and measurement are observed to be quite good.

EPNL Sensitivity Study

To assess the inflight signature of coannular plug nozzle jet mixing and shock noise, flight effects were applied to the measured engine noise data scaled to a product engine size. Several methods were used in this sensitivity study (see References 8 to 10). Figure 23 illustrates the projected EPNL's for a typical sideline noise condition. Table 2 gives the projected differences in EPNL between the conic nozzle and the coannular plug nozzle for typical sideline, cutback and approach conditions for the test points described in Table 3. This sensitivity study showed that regardless of the methods used, the projected variations in EPNL were not large at all ($\sim \pm$ 1.5 EPNL), and

that typical EPNL differences between the conic nozzle and coannular plug nozzle are about 5-6 EPNL.

VERIFICATION OF FLIGHT JET NOISE REDUCTION FROM RECENT MODEL SCALE FREE-JET TESTS

To substantiate flight jet noise reduction for coannular plug nozzles, free-jet acoustic measurements were taken at General Electric's anechoic facility. A similitude model of the YJ101 R_r^o = .853, A_r^i =.2 coannular plug nozzle was tested. Sample test results verifying coannular plug nozzle flight jet noise reduction is given in Figures 24 and 25.

Shown in Figure 24 is a comparison between a conic nozzle and a coannular plug nozzle (R_r^o =.853, A_r^i =.2) at a free jet velocity of 122 m/sec (400 fps) at typical takeoff sideline engine cycle condition. The measurements indicate that coannular jet and shock noise reduction is maintained at all observation angles. Figure 25 presents the measured flight spectral suppression trends at θ_i=60°, 90°, 140°. At all angles the coannular plug nozzle shows flight reduction of the same order as observed from previous static tests.

OTHER ENGINE TEST RESULTS

In addition to the far-field jet engine acoustic measurements described above, diagnostic measurements were performed. These measurements included sample fan inlet noise measurements, laser velocimeter measured mean velocity and turbulent velocity profiles, peak noise source locations from traversing microphone measurements, and core noise measurements. A brief summary of these results is given below.

Measurements of YJ101 Fan Inlet Turbomachinery

For one series of YJ101 conical nozzle engine tests, the treated inlet was removed and tests were performed with a standard untreated bellmouth inlet. Figure 26 illustrates these results. Although the noise signature is strongly influenced by the conic nozzle jet and shock noise (at high power settings), the fan noise tone characteristics indicate the difference tone generated from stage 1 to 2 or 2 to 3 strongly influences the forward quadrant fan spectrum and PNL. However, the YJ101 fan inlet noise for these tests were found to be within previously measured fan data sources. Figure 27 compares these YJ101 fan inlet measurements relative to several other data sources.

Laser Velocimeter Measurements of YJ101 Engine Exhaust Plumes

The General Electric Company has developed a unique velocity measurement capability for both laboratory and engine diagnostic measurements. (See Reference 1 and 11 to 13 for description of the LV system and its application to model scale jet exhaust tests).* Figure 4 shows the laser velocimeter system which was used for the YJ101 engine measurements. This same laser/processor system is used for all G.E. laboratory diagnostic testing.

Figures 28 and 29 illustrate respectively typical mean velocity radial profile measurements for the conical nozzle and the coannular plug nozzle engine test measurements. The observed feature is that for the baseline conical nozzle a rather normal velocity profile was measured.* For the coannular nozzle the inner and outer stream for the coannular plug nozzle system is fully identified - at supercritical, high temperature conditions.

Figures 30 and 31 show comparisons of laser velocimeter measured mean and turbulent velocities for model scale and YJ101 engine tests. The results of Figure 30 clearly show the shock structure of the conic nozzle and the relatively low exit plane exhaust turbulence levels of the YJ101 engine. Figure 31 shows a favorable comparison for the axial mean velocity decay of the coannular plug nozzle between model and YJ101.

Sideline Traverse Test Results and Core Noise Measurements

From the sideline traverse microphone measurements (See Figure 5 for test set-up), the axial location of each 1/3 octave band peak noise source can be deduced. Figure 32 shows a comparison of the Strouhal distribution of peak noise source locations and far-field radiation angles for YJ101 conical nozzle measurements compared with other data sources. The general results obtained were that the high frequency noise sources are close to the nozzle exit and the lower frequency sources are further downstream. These results compare with previously measured test experiences using a J79 engine. Coannular plug nozzle tests showed that the higher frequency noise sources are closer to the nozzle exit than are the conic nozzle (See Reference 3 for additional details).

* An answer desired from the laser measurements was whether the YJ101 engine conic nozzle (which mixed the fan by-pass air into the core stream with a series of 24 aft variable area by-pass injectors) would have a fully mixed exit velocity profile, or some other profile which could lend to an erroneous type of baseline for acoustic measurements. The laser tests (as well as our scaling tests)show that the baseline conic nozzle was a valid baseline.

Core Engine Noise Results

From internal kulite measurements and cross-correlation techniques, YJ101 core exhaust noise measurements were performed. The results were that the internal noise sources did not contaminate any of the jet noise measurements made in the far-field or nearfield. (Reference 3 contains the detailed measurements which lead to this conclusion.)

POSSIBILITIES FOR ADDITIONAL JET NOISE REDUCTION

The acoustic measurements obtained from the YJ101 engine tests and free-jet acoustic model scale tests indicate that FAR36 (1969) type noise level technology may be possible for SCR type aircraft. There are, however, possibilities of achieving additional jet noise reductions as follows:

1. Engine cycle and engine sizing

   Fan oversizing benefit - 1-2 EPNdB reduction identifiable for the sideline.

   Engine high flow benefit - 1.5- 3 EPNdB reduction at the community measurement point is possible.

2. Advanced Aircraft Operational Procedures -

   1-2 EPNdB reduction can be expected.

3. Mechanical Suppression for Coannular Plug Nozzles - Up to 5 EPNdB reduction relative to the unsuppressed high-radius-ratio coannular plug nozzle is believed achievable; simple in mechanical design, lightweight, and with only $\sim$ 4% additional nozzle performance loss.

4. The use of Alternative Jet and Shock noise reduction schemes, such as engine mounting; application of a thermal acoustic shield or a mechanical treated ejector; enhanced exhaust mixing concepts such as coplanar mixer and tangential flow schemes; and viable combination of the above.

Tables 4 and 5 summarize some of these possibilities. Although the achievement of all the above items have not been demonstrated in a collective manner, 1979 work efforts show that the outlook for achieving noise levels approaching FAR36(1978) Stage 3 is encouraging.

As examples of recent NASA/GE contract efforts (NAS3-21608) and General Electric supported efforts, Figures 33, 34, and 35 are shown. Figures 33 and 34 show the acoustic and projected aerodynamic performance of a simple 20 shallow chute mechanical coannular plug nozzle suppressor. The results show that relative to a conical nozzle baseline, up to 11.5 PNdB reduction is possible at the sideline noise measurement location. As an example of 'alternative' jet noise suppression schemes, Figure 35 presents model scale free-jet measurements illustrating flight suppression achieved using a high-radius-ratio plug nozzle with a low velocity, high temperature thermal acoustic shield.* The results show up to 5 PNdB flight jet noise suppression relative to the core nozzle.

CONCLUDING REMARKS

The results of the YJ101 engine and model scale free-jet acoustic test results have shown that a significant amount of acoustic technology advancement has been achieved for Advanced Supersonic Cruise type aircraft.

From the Static YJ101 VCE Engine Test Program:

- For the first time anywhere, rather comprehensive advanced acoustic (far-field, nearfield, probe, and coherence) measurements were successfully and systematically performed on a high performance VCE engine test vehicle with a high-radius-ratio coannular plug nozzle.
- Significant static jet noise reduction (4-6 PNdB peak aft angle) and shock noise reduction ($\sim$ 7 PNdB) was demonstrated for General Electric's high-radius-ratio coannular plug nozzle.
- Scale model and engine jet noise scaling laws for coannular plug nozzles appeared verified.
- A unique spectral prediction method of jet and shock noise for coannular plug nozzles was successfully developed and illustrated.
- Probe and coherence measurements show no significant core noise contribution relative to the jet noise.
- Typical supersonic three (3) stage closely coupled fan noise was measured - Inlet radiated noise was approximately 5 PNdB higher than high by-pass fans under static conditions.

* The Boeing Airplane Company has done extensive prior testing of such an alternative suppression concept. These results however, are believed to be the first free-jet evaluation for a SCR type engine application.

- Extensive laser velocimeter mean velocity and turbulence velocity measurements were acquired. The YJ101 engine exhaust plane turbulence levels were measured to be relatively low ($\sim$ 4%). Comparison of engine measurements with model scale measurements were very good.

From model scale free-jet measurements:

- Flight suppression for the unsuppressed coannular plug nozzle was verified. Up to 5 EPNdB relative to a fully mixed conical nozzle is believed to be achievable at typical take off power and cut-back conditions.

- Options for obtaining additional jet and shock noise reductions were identified:

    1. A shallow chute mechanical suppressor (up to 11.5 peak static PNdB reduction relative in baseline conic nozzle)- simple mechanical design, lightweight; $\sim$ 4% flight performance loss relative to the unsuppressed coannular plug nozzle.

    2. Alternative jet noise abatement schemes:

        - thermal acoustic shield
        - enhanced internal mixing schemes
        - appropriate combinations of alternative schemes and simple mechanical suppressor concepts.

Although additional work is still necessary, the outlook for achieving SCR aircraft noise levels on the order of current subsonic commercial airplanes is good. Appropriate engine and free-jet model scale programs should be continued, the goal of which should be to provide the technology to achieve FAR36(1978) Stage 3 noise levels or an appropriate equivalent (e.g., sum of three point requirements).

In terms of "next steps" for advancements in acoustic technology, the following items are recommended.

1. Establish a SCR Government/Industry noise technology goal- meet FAR36(1978) Stage 3 or an appropriate equivalent goal which properly accounts for the unique characteristics of a supersonic cruise type aircraft.

2. Continue use of the YJ101/VCE as an engine acoustic test vehicle.

- Mechanical Suppressors

- Inlet Noise Studies

- Demonstration of alternative jet noise abatement schemes

- Simulated flight tests of coannular nozzles and simple coannular suppressors, including inlet fan noise reduction devices (NASA Ames 40 X 80 Wind Tunnel).

3. Continue with aggressive and probing model scale free-jet acoustic and aerodynamic performance research investigations. Emphasis of these programs should be: to formulate appropriate suppressor theoretical prediction models; screening type testing for eventual engine evaluation; free-jet (flight) noise evaluation of all selected concepts; carry out dual paths of investigation - 1. Classical mechanical suppressors 2. Alternative schemes; research efforts which have a greater emphasis on shock noise control schemes. The end objective would be to achieve equivalent subsonic airplane noise levels without significant adverse impact on fuel and airplane economics.

REFERENCES

1. Knott, P.R., Stringas, E.J., Brausch, J.F., Staid, P.S., Heck, P.H., Lathem, D., Acoustic Tests of Duct-Burning Turbofan Jet Noise Simulation NASA CR 2966 (July 1978).

2. Knott, P.R., Blozy, J.T., Staid, P.S., Acoustic and Aerodynamic Performance Investigation of Inverted Velocity Profile Coannular Plug Nozzles, NASA CR 3149 (June 1979).

3. Savell, C.T., Stringas, E.J. et.al., High Velocity Jet Noise Source Location and Reduction Task I - Activation of Facilities and Validation of Source Location Techniques FAA-RD-76-79, I (February 1977).

4. Ibid, Task I Supplement - Certification of the General Electric Jet Noise Anechoic Test Facility FAA-RD-76-79, Ia (February 1977).

5. Clapper, W.S., Stringas, E.J. et.al., High Velocity Jet Noise Source Location and Reduction Task 5 - Investigation of In-Flight Aeroacoustic Effect on Suppressed Exhuasts, FAA-RD-76-79 V (January 1979).

6. Lee, R., Coannular Plug Nozzle Noise Reduction and Impact on Exhaust System Designs, Proceedings of the SCAR Conference November 1976, NASA CP-001, p 505, Part II.

7. Bhutiani, P.K., A Unique Coannular Plug Nozzle Jet Noise Prediction Procedure, General Electric TIS R 79 AEG 481, October 1979.

8. FAA-RD-76-79, II, High Velocity Jet Noise Source Location and Reduction - Task 2, October, 1977.

9. FAA-RD-76-79, VI, High Velocity Jet Noise Source Location and Reduction - Task 6, April, 1979.

10. Stone, J.R., An Improved Method for Predicting the Effects of Flight on Jet Mixing Noise. NASA TM-79155, 1979.

11. Benzakein, M.J., Knott, P.R., "Supersonic Jet Exhaust Noise," AFAPL - TR-82-52, August 1972.

12. Knott, P.R., et.al., "Supersonic Jet Exhaust Noise Investigation", AFAPL-TR-76-68 July 1976.

13. Knott, P.R., Scott, P.F., Mossey, P.W., High Velocity Jet Noise Source Location and Reduction Task 3 - Experimental Investigation of Suppression Principles Volume IV - Laser Velocimeter Time Dependent Cross Correlation Measurements FAA-RD-76-79, III-IV (December 1978).

TABLE 1

Band No. i	17 to 30	31	32	33	34	35	36-43
1/3 O.B. Ctr. Freq.	50Hz to 1kHz	1.25kHz	1.6kHz	2.0kHz	2.5kHz	3.15kHz	4 to 10kHz
Weighting Factors	R_i 1.0	.83	.67	.5	.33	.17	0.0
	S_i 0.0	.17	.33	.5	.67	.33	1.0

TABLE 2.- PROJECTED DIFFERENCE IN EPNL BETWEEN THE CONIC NOZZLE AND COANNULAR PLUG NOZZLE AT TYPICAL SIDELINE, CUT-BACK AND APPROACH CONDITIONS

METHOD	EPNL conic* − EPNL coannular			
	SIDELINE, EPNdB	SIDELINE, EPNdB	CUT-BACK, EPNdB	APPROACH, EPNdB
M J T SMITH	5.1	6.05	4.53	1.72
BUSHELL	5.6	6.65	4.43	2.42
HOCK (SAE)	4.8	5.85	3.93	1.82
TASK 6	4.7	5.15	4.23	1.52
MGB	5.1	6.05	4.23	2.02

*CONIC NOZZLE CONDITIONS CORRECTED TO MATCH COANNULAR PLUG NOZZLE V_j^{mix}, P_j^{mix} AND A_T.

TABLE 3.- TEST CONDITIONS FOR EPNL PROJECTIONS

TYPE CASE	Test P+	V_j^o m/sec (ft/sec)	T_t^o ^oK (^oR)	P_r^o	V_j^i m/sec (ft/sec)	T_t^i ^oK (^oR)	P_r^i	V_j^{mix} m/sec (ft/sec)	Acoustic Range m (ft)
SIDELINE	329	751.94 (2467)	1065.55 (1918)	2.87	484.63 (1590)	473.88 (853)	2.695	692.38 (2272)	731.52
	413	693.72 (2276)	992.22 (1786)	2.591	450.19 (1499)	446.67 (804)	2.45	639.56 (2098)	731.52
CUT-BACK	324	547.72 (1797)	868.88 (1564)	1.92	369.72 (1213)	415.00 (747)	1.87	508.10 (1667)	304.8 (1000)
APPROACH	288	381.00 (1250)	715.55 (1288)	1.49	277.97 (912)	371.11 (668)	1.47	368.19 (1208)	112.77 (370)

TABLE 4.- POSSIBILITIES FOR ADDITIONAL JET NOISE REDUCTION

1. ENGINE OVERSIZING; CYCLE AND HIGH FLOWING ADVANCEMENTS

   - OVERSIZING (SIDELINE) - 1-2 EPNDB REDUCTION

   - HIGH FLOW AND CYCLE OPTIMIZATION (COMMUNITY) - 1.5 - 3 EPNDB

2. ADVANCED AIRCRAFT OPERATIONAL PROCEDURES - NASA LANGLEY AND OTHERS

   - GENERALLY ACCEPTED THAT 1-2 DB BENEFIT CAN BE EXPECTED

3. GE COANNULAR PLUG NOZZLE MECHANICAL SUPPRESSORS

   - UP TO 5 EPNDB REDUCTION OVER UNSUPPRESSED COANNULAR PLUG NOZZLE IS CURRENT GOAL

4. ALTERNATIVE JET NOISE ABATEMENT SCHEMES

   - 3 TO 8 PNDB POSSIBLE

   - THERMAL ACOUSTIC SHIELDS, INTERNAL/COPLANAR MIXERS, TREATED EJECTORS

   - COMBINATIONS OF MECHANICAL SUPPRESSORS AND ALTERNATIVE SCHEMES

TABLE 5.- PROJECTED NOISE LEVELS INCORPORATING ADVANCED FEATURES[1] - 750 KLB TOGW

	BASELINE[2]	MECHANICAL SUPPRESSOR	HIGH FLOW & OVERSIZED FAN (20%)	ADVANCED A/C OPERATIONAL PROCEDURES	REDUCED NOISE LEVEL	FAR36(1978)
SIDELINE	112	-5	-1.5	-1.0	104.5	102.5
COMMUNITY	110.5	-3	-3.0	-1.5	103.0	105.5
APPROACH	104.5	-	-	-	104.5	105.5

(1) COMPLETE ENGINE/AIRPLANE SYSTEMS STUDY WITH ALL THE ABOVE ADVANCED FEATURES HAS NOT BEEN DONE.

(2) 4 GE21/J11B9 ENGINES WITH A HIGH-RADIUS-RATIO COANNULAR PLUG NOZZLE; PARTIAL CHOCKED INLET; 10% OVERSIZED FAN; MONITORING POINTS ARE FOR FAR36(1978) STAGE 3.

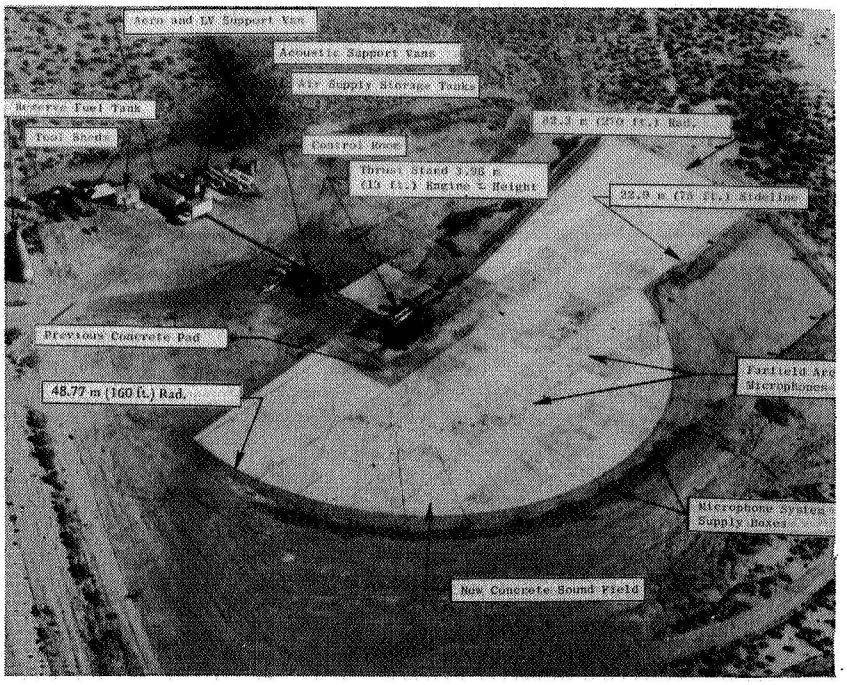

Figure 1.- Layout of Edwards test site.

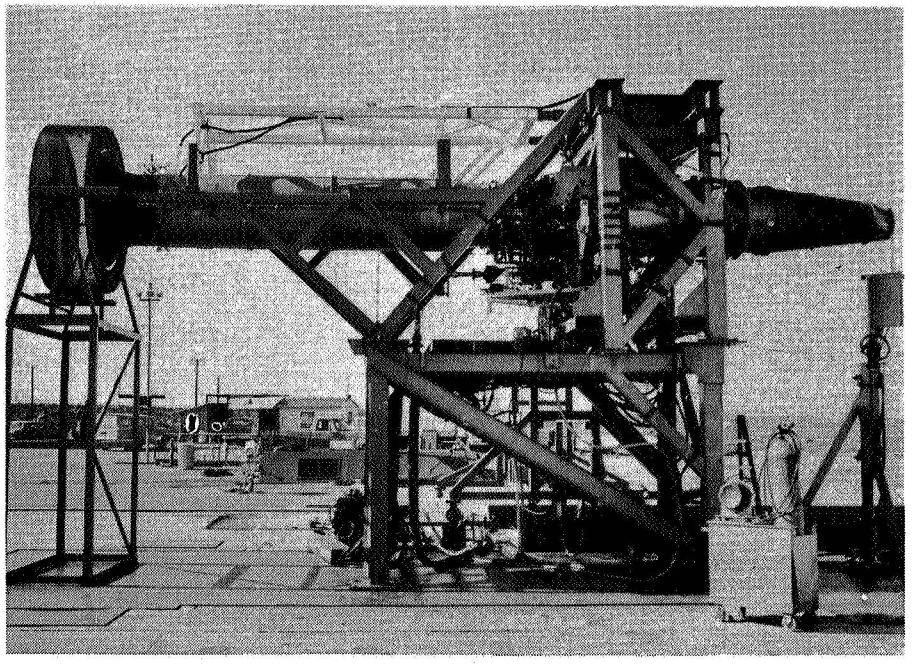

Figure 2.- YJ101 engine conic nozzle with treated fan inlet.

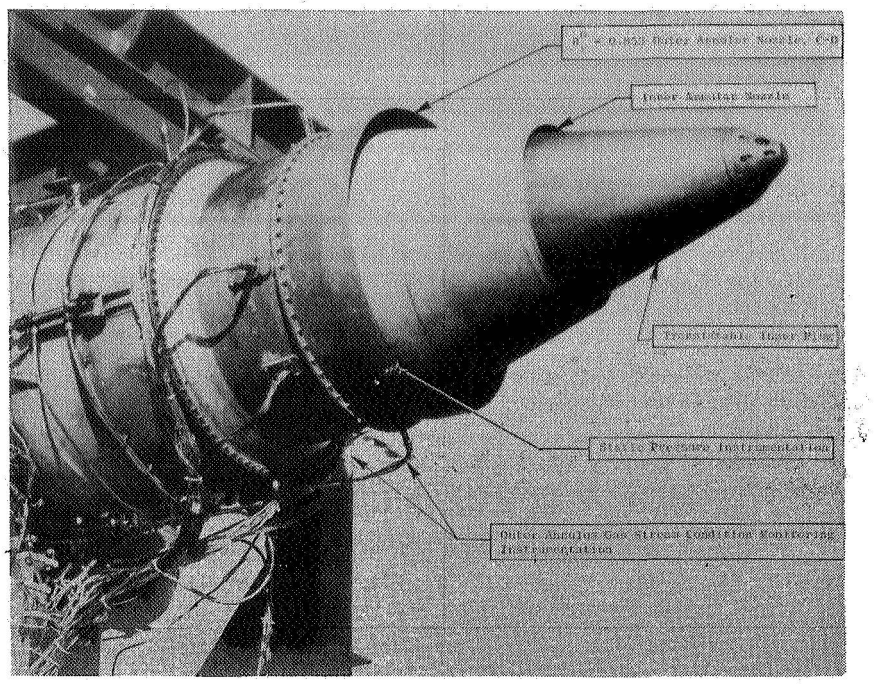

Figure 3.- Photo of coannular plug nozzle.

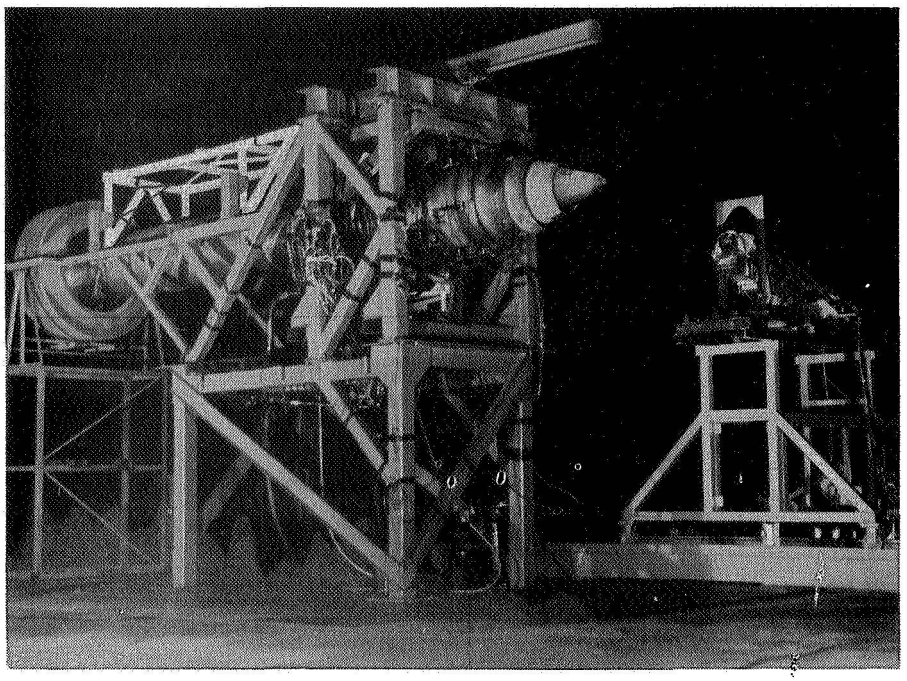

Figure 4.- YJ101 coannular plug nozzle test vehicle with G.E. laser velocimeter.

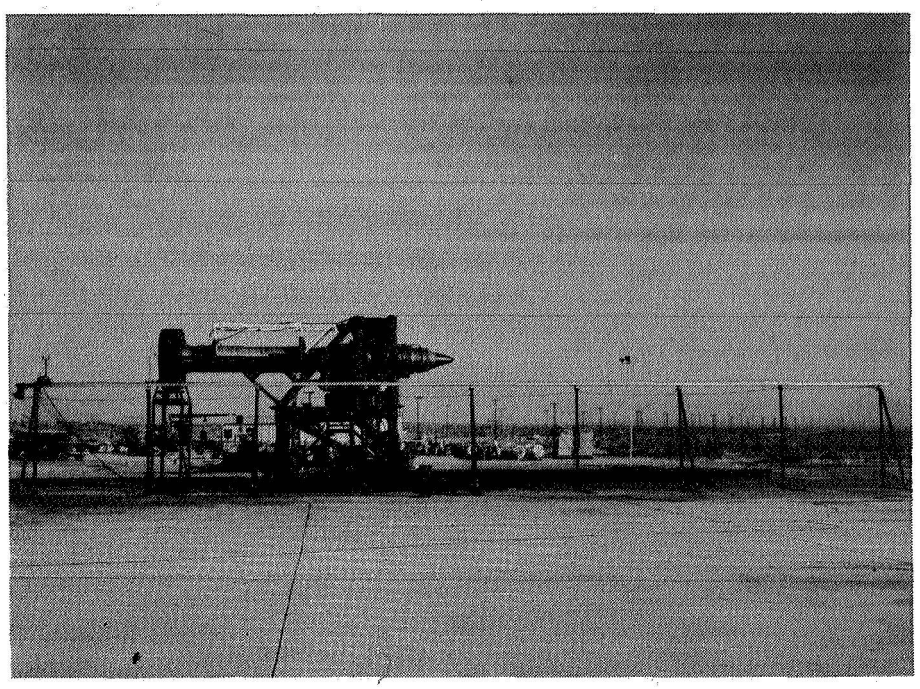

Figure 5.- YJ101 acoustic test vehicle with NASA Ames traversing microphone system.

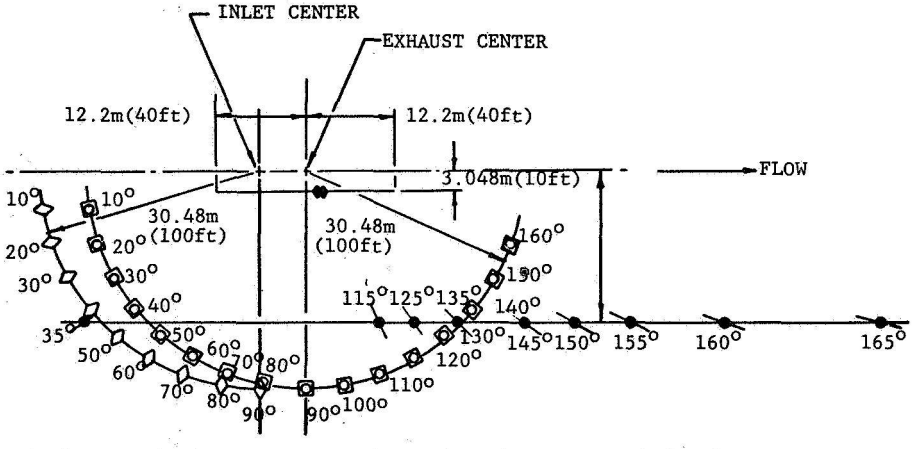

SYMBOL	MICROPHONE ORIENTATION	MEASUREMENT DISTANCE	TYPE OF MICROPHONE ARRAY	CENTER OF RADIAL MEASUREMENTS
●	GROUND	21.34m(70ft)	SIDELINE	
○	GROUND	30.48m(100ft)	ARC	EXHAUST NOZZLE
□	ENGINE CENTERLINE	30.48m(100ft)	ARC	EXHAUST NOZZLE
◇	ENGINE CENTERLINE	30.48m(100ft)	ARC	INLET
—◆—	ENGINE CENTERLINE	30.48m(10ft)	SIDELINE	

Figure 6.- Layout of Edwards test site.

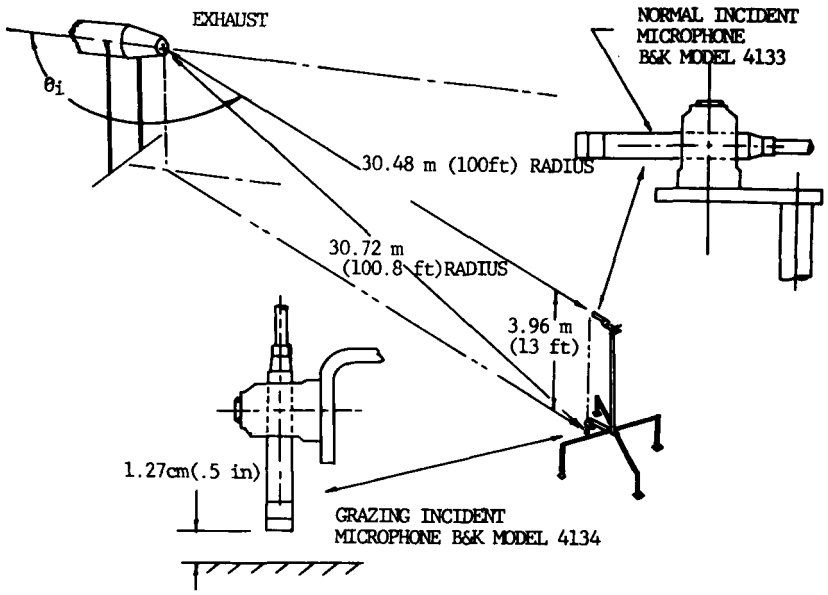

Figure 7.- Illustration of microphone setup.

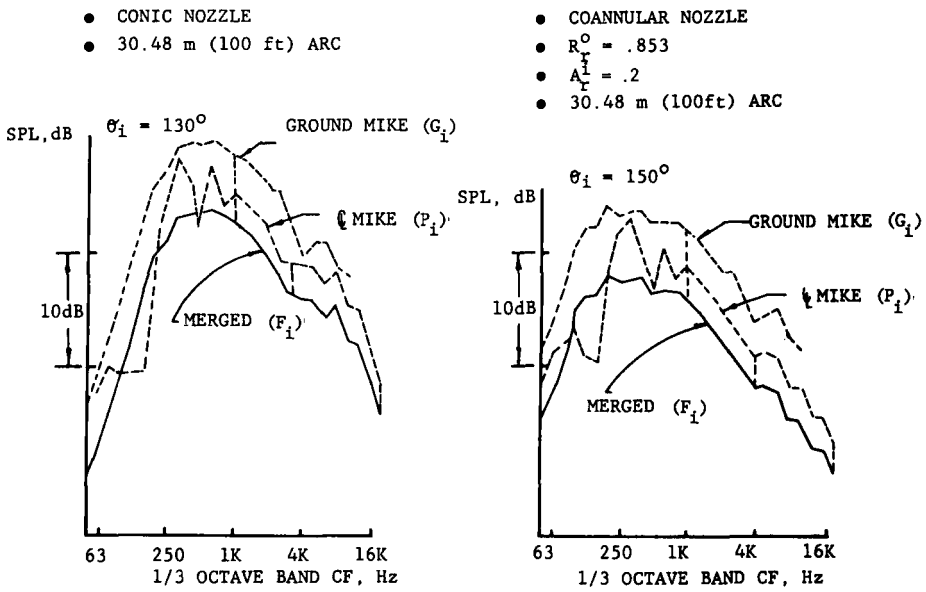

Figure 8.- Illustration of spectral merging.

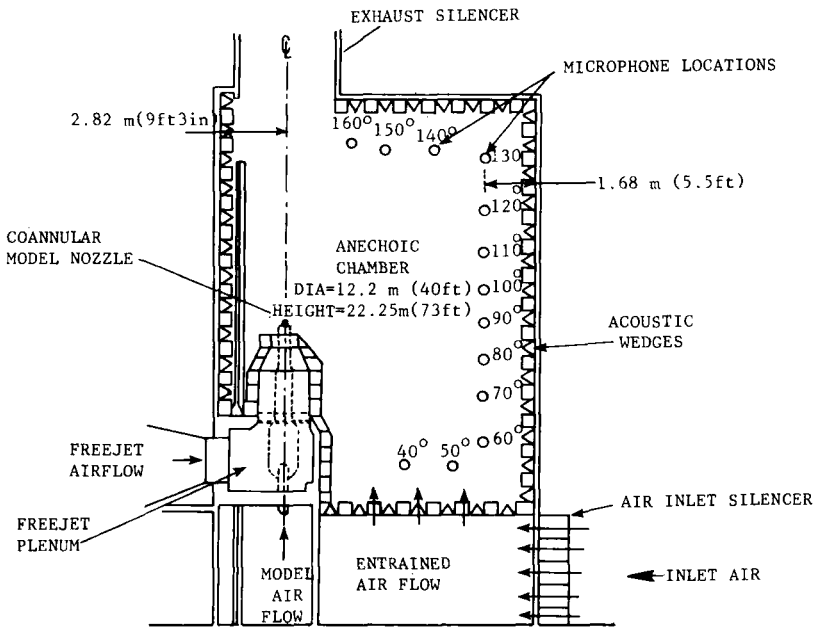

Figure 9.- Schematic of General Electric anechoic free-jet facility.

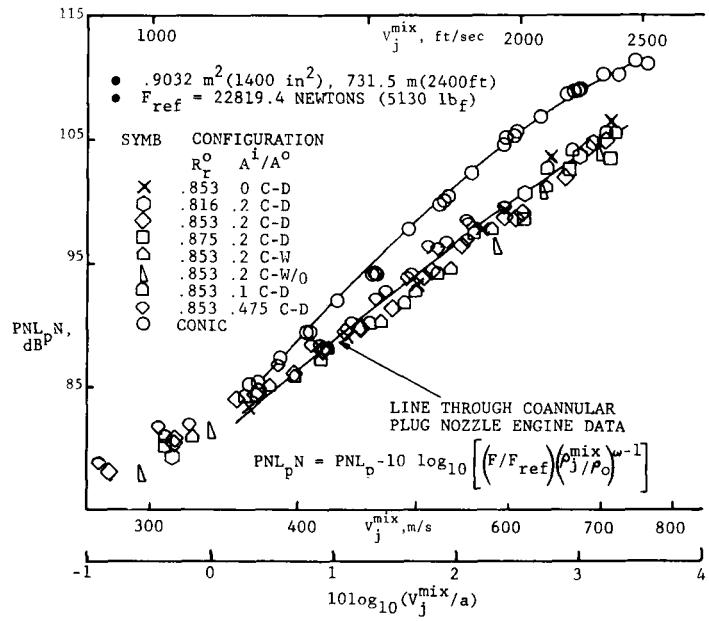

Figure 10.- Verification of coannular plug nozzle engine jet noise reduction.

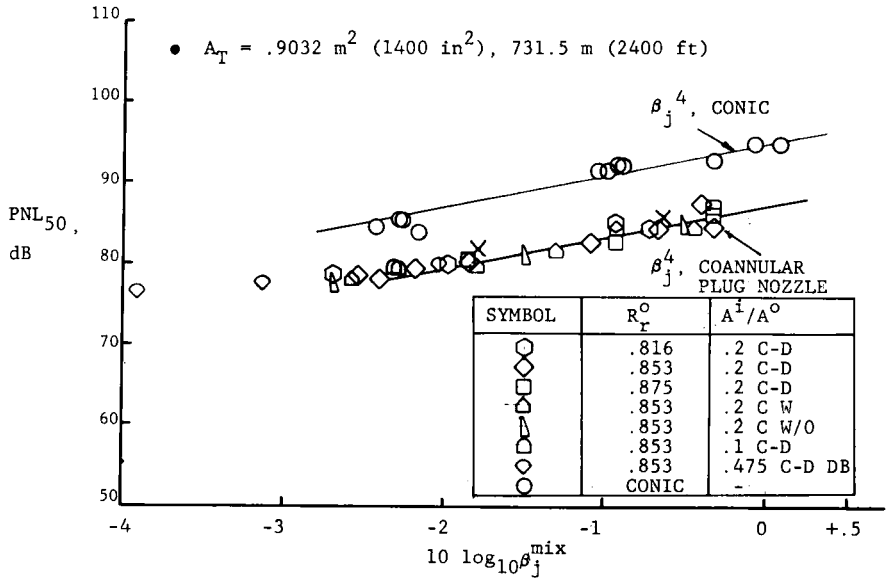

Figure 11.- Verification of coannular plug nozzle engine shock noise reduction.

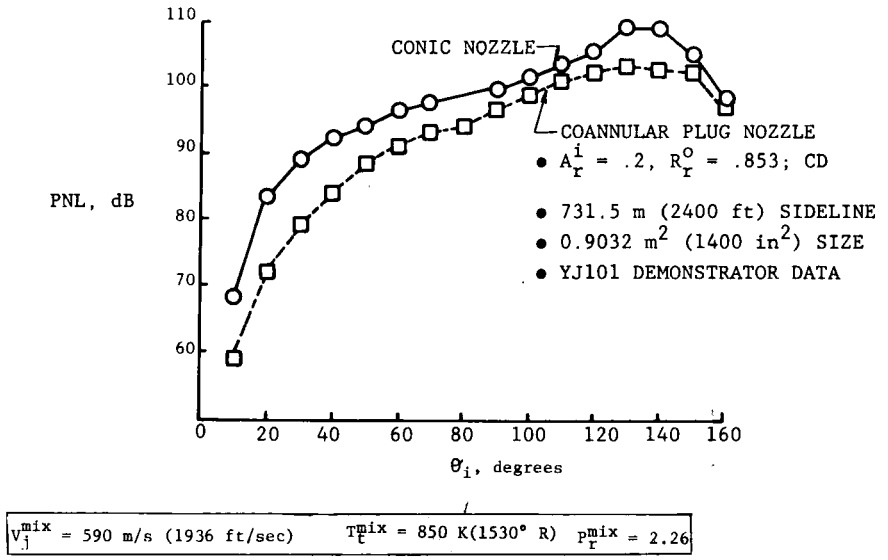

Figure 12.- Typical engine PNL directivity — conic and coannular plug nozzle.

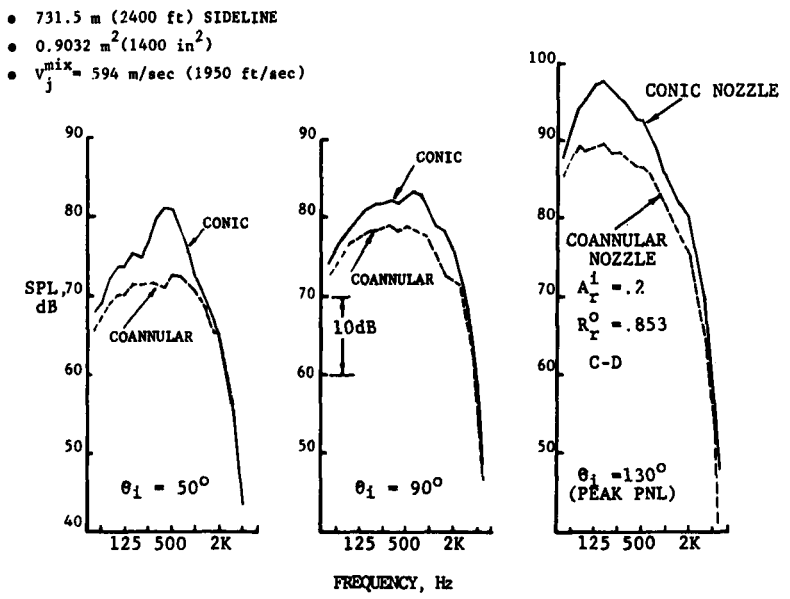

Figure 13.- Typical engine spectra characteristics — conical and coannular plug nozzle.

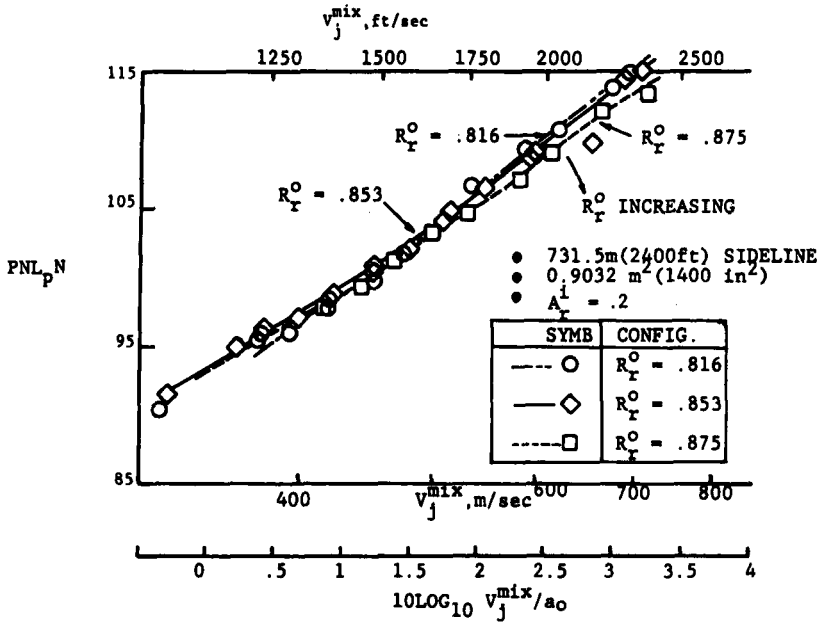

Figure 14.- Influence of radius ratio effects on coannular plug nozzle jet noise reduction.

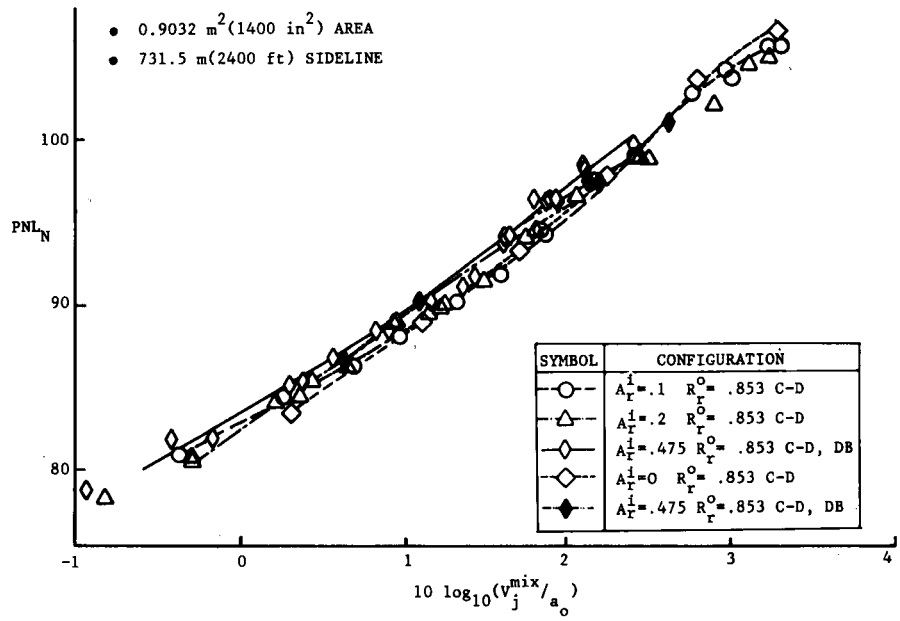

Figure 15.- Influence of area ratio effects on coannular plug nozzle jet noise reduction.

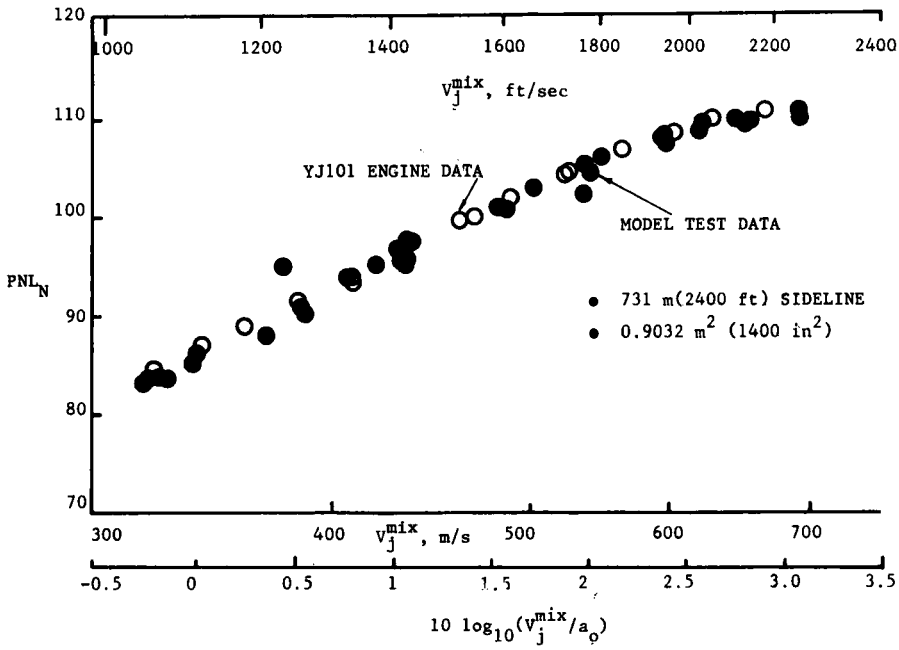

Figure 16.- Conical nozzle peak PNL acoustic scaling comparison.

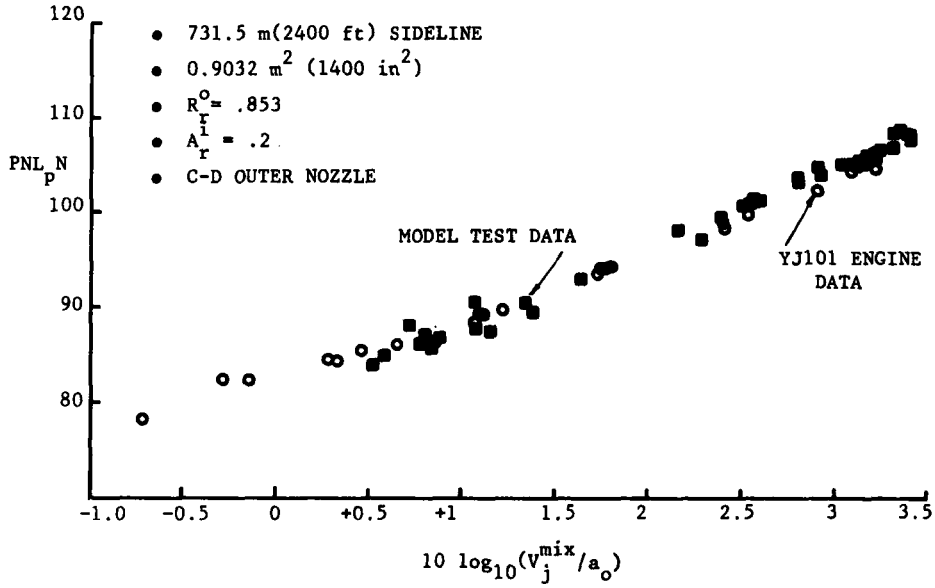

Figure 17.- Coannular plug nozzle peak PNL acoustic scaling comparison.

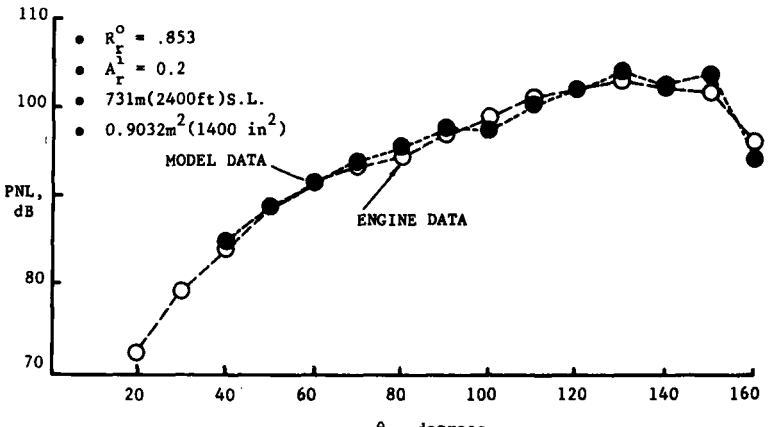

	V_j^o,m/sec (ft/sec)	T_T^{mix},K (^oR)	P_r^o	V_j^i,m/sec (ft/sec)	T_T^o,K (^oR)	P_r^i	V_j^{mix},m/sec (ft/sec)	T_t^{mix}K (^oR)	P_r^{mix}
J101	640.38 (2101)	957 (1723)	2.278	421 (1382)	440 (793)	2.181	594 (1950)	849 (1528)	2.261
MODEL	643 (2110)	958 (1724)	2.307	389 (1276)	398 (716)	2.084	588 (1930)	678 (1220)	2.223

Figure 18.- Coannular plug nozzle scaling — PNL directivity.

	V_j^o, m/s (ft/sec)	T_T^o,K (^oR)	P_r^o	V_j^i, m/s (ft/sec)	T_T^i,K (^oR)	P_r^i	V_j^{mix}, m/s (ft/sec)	T_T^{mix},K (^oR)	P_r^{mix}
YJ101 MODEL	640 (2101)	957 (1723)	2.278	421 (1382)	440 (793)	2.181	594 (1950)	849 (1528)	2.261
	643 (2110)	958 (1724)	2.307	389 (1276)	398 (716)	2.084	588 (1930)	678 (1220)	2.223

- 731m(2400 ft) SIDELINE
- 0.9032 m^2(1400 in^2)

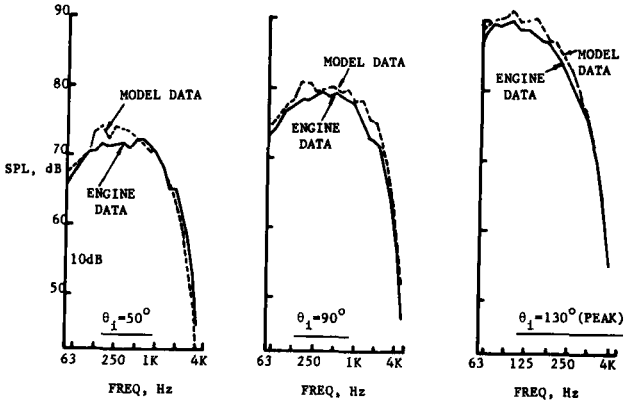

Figure 19.- Conical plug nozzle scaling — SPL spectra.

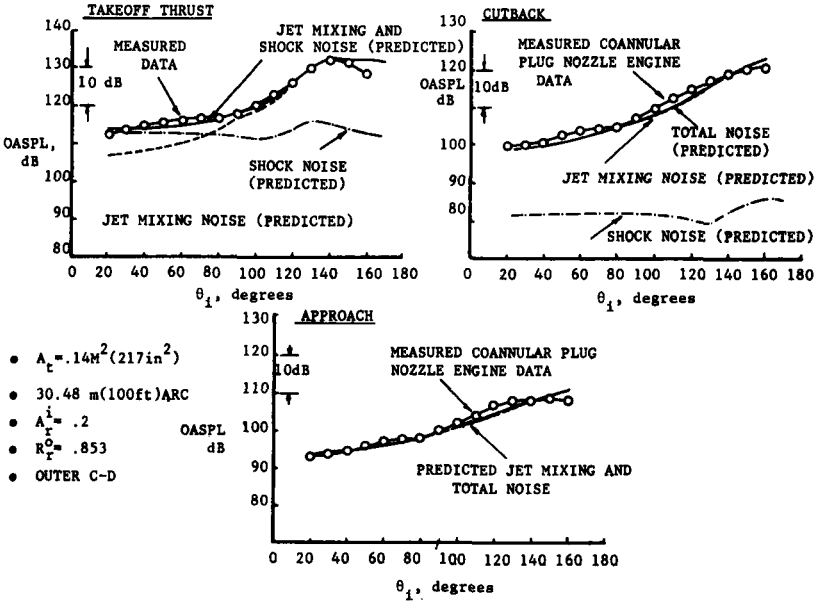

Figure 20.- Theory data comparison for engine coannular plug nozzle jet mixing and shock noise — OASPL directivity.

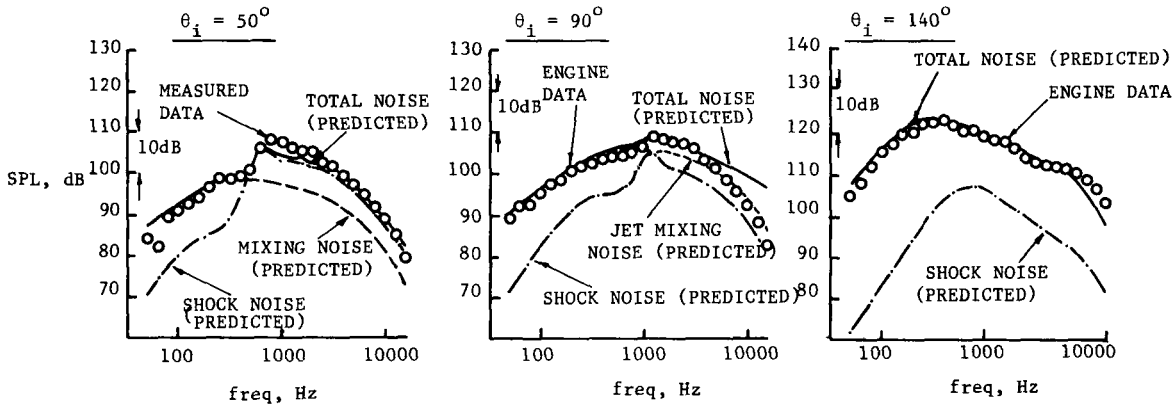

V_j^o, m/sec (ft/sec)	T_T^o, K (^oR)	P_r^o	V_j^i, m/sec (ft/sec)	T_T^i, K (^oR)	P_r^o	V_j^{mix}, m/sec (ft/sec)	T_T^{mix}, K (^oR)	P_r^{mix}
777 (2548)	1084 (1969)	3.0	498 (1633)	478 (861)	2.84	714 (2342)	955 (1719)	2.9

Figure 21.- Theory data comparison for engine coannular plug nozzle jet mixing and shock noise — SPL spectra (typical SL condition).

- 30.48 m(100 ft)
- DEMO SIZE .14m^2(217 in^2)
- A_r^i = .2
- R_D^o = .853
- C-D OUTER NOZZLE

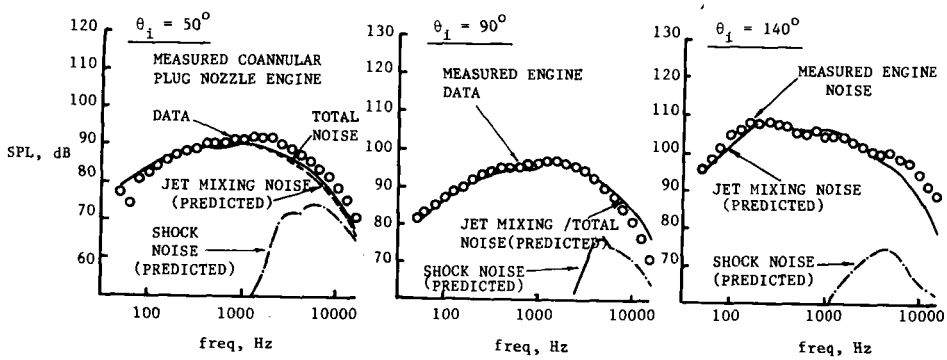

V_j^o, m/sec (ft/sec)	T_t^o, K (^oR)	P_r^o	V_j^i, m/sec (ft/sec)	T_t^i, K ^oR	P_r^i	V_j^{mix}, m/sec (ft/sec)	T_t^{mix}, K (^oR)	P_r^{mix}
548 (1797)	869 (1564)	1.923	370 (1213)	415 (747)	1.871	508 (1666)	767 (1381)	1.890

Figure 22.- Theory data comparison for engine coannular plug nozzle jet mixing and shock noise — SPL spectra (typical C-B condition).

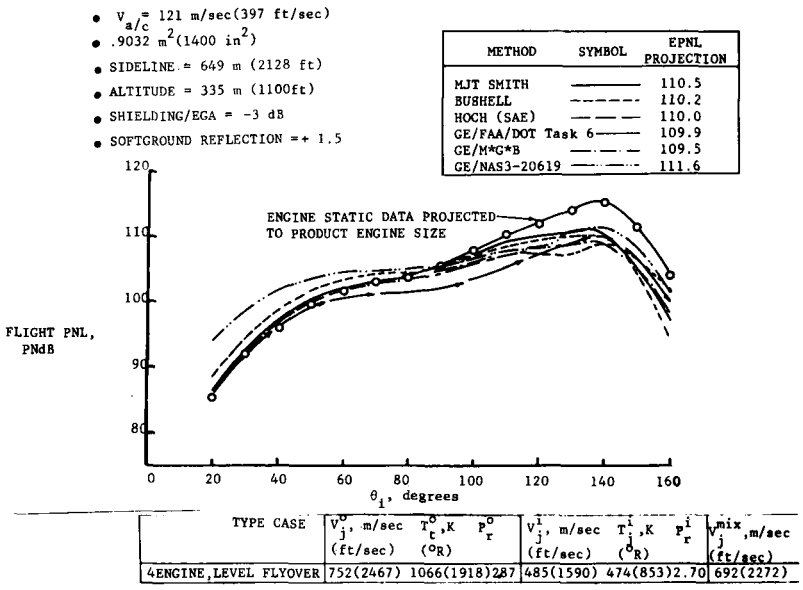

Figure 23.- Projected flight jet and shock noise for a high radius ratio coannular plug nozzle using several flight effects methods at a typical sideline condition.

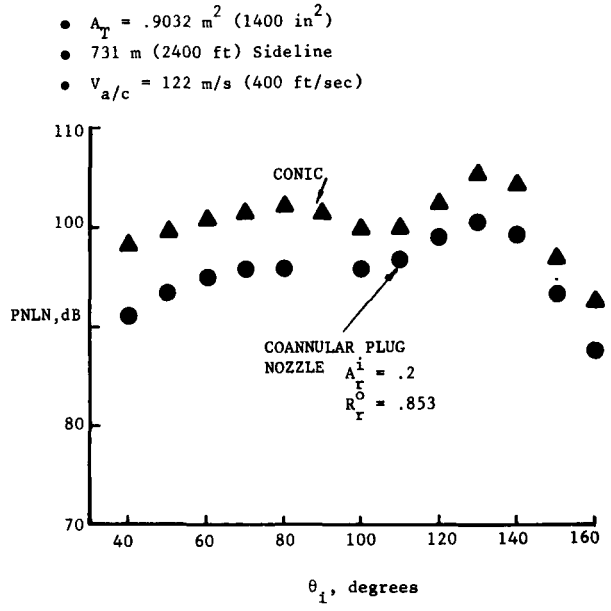

Figure 24.- Verification of flight suppression for coannular plug nozzles — PNL directivity comparison.

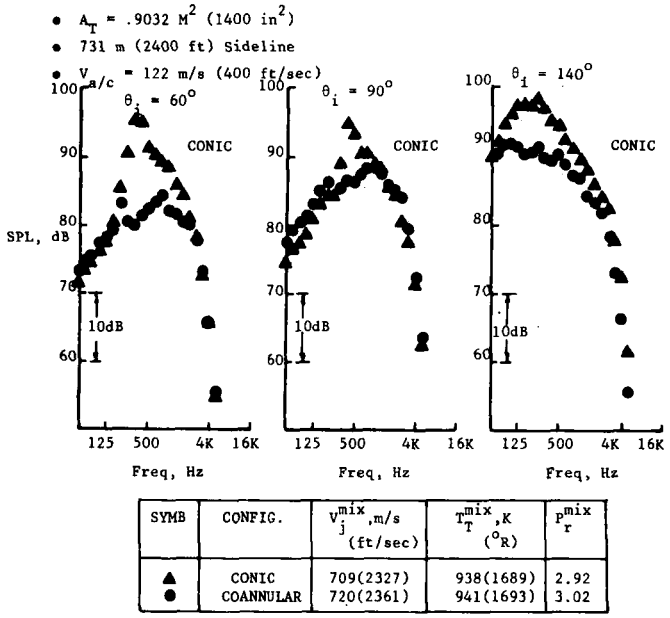

SYMB	CONFIG.	V_j^{mix}, m/s (ft/sec)	T_T^{mix}, K (^oR)	P_r^{mix}
▲	CONIC	709(2327)	938(1689)	2.92
●	COANNULAR	720(2361)	941(1693)	3.02

Figure 25.- Verification of flight suppression for coannular plug nozzles — SPL spectra comparisons.

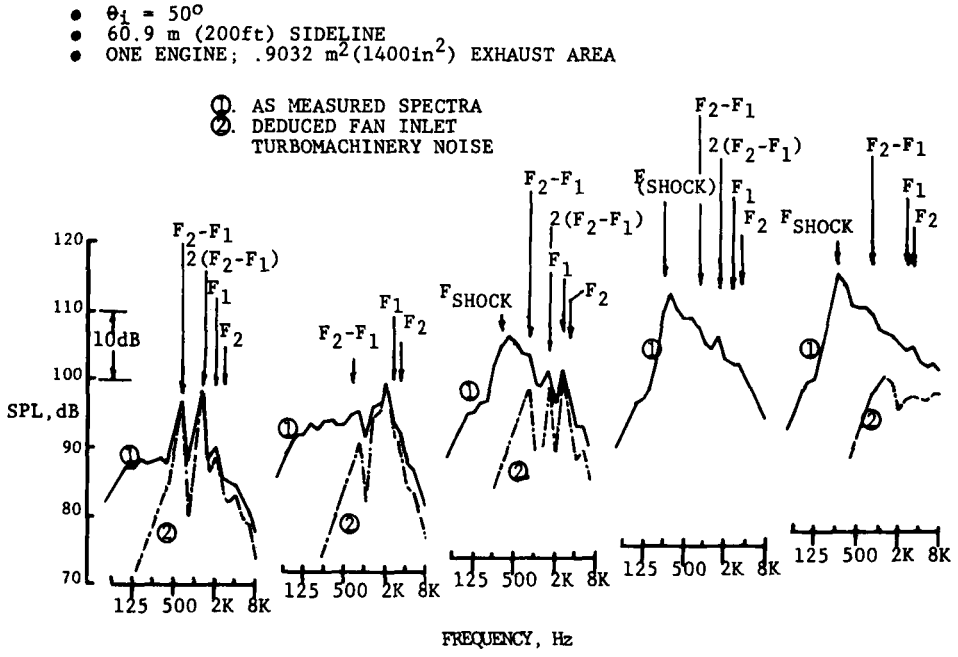

Figure 26.- Typical fan inlet turbomachinery noise.

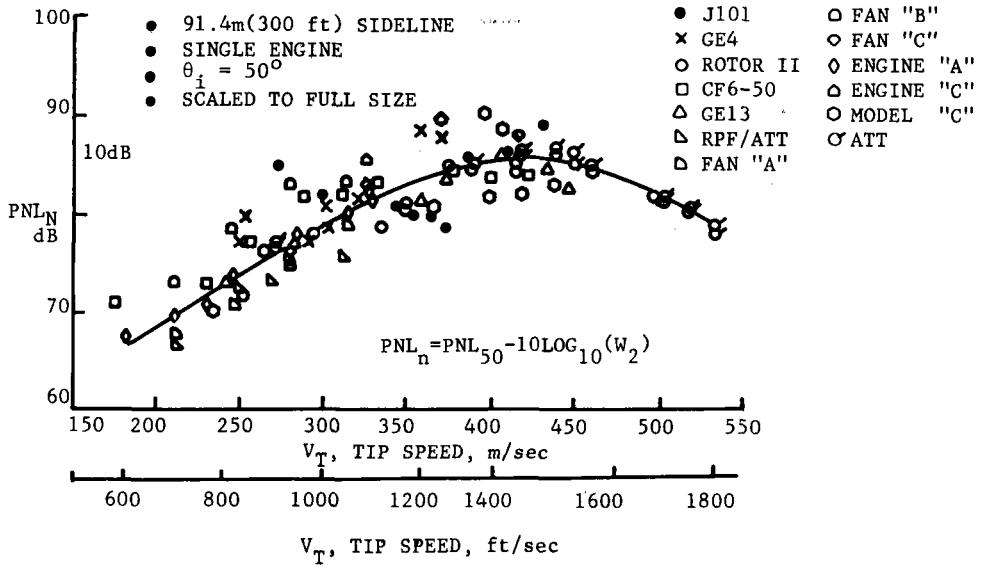

Figure 27.- YJ101 fan inlet noise relative to other data sources.

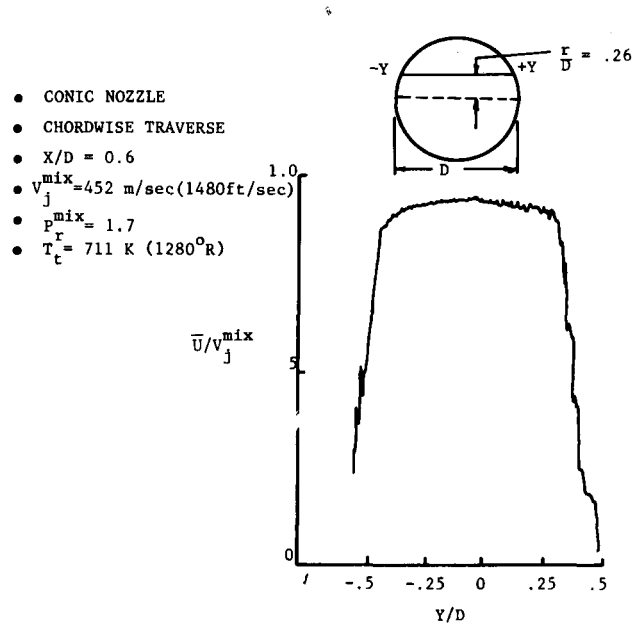

Figure 28.- Typical laser velocimeter measured mean velocity profile for engine conical nozzle tests – subsonic jet.

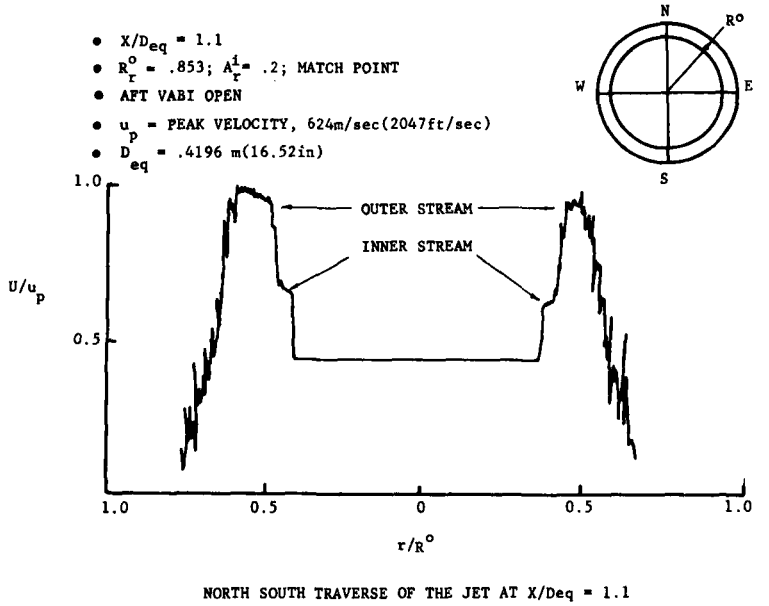

Figure 29.- Typical laser velocimeter measured mean velocity profile for engine coannular plug nozzle tests — supersonic conditions.

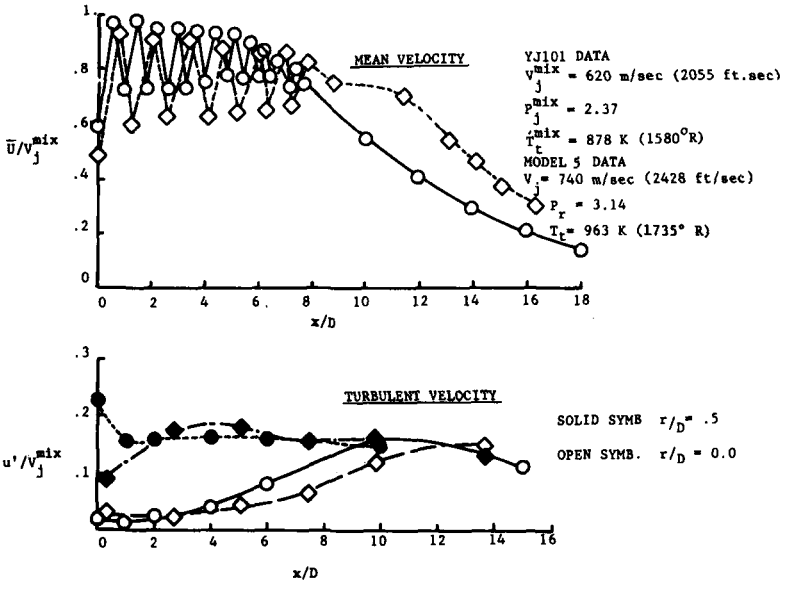

Figure 30.- Comparison of laser velocimeter measured mean velocity and turbulent velocity distributions between engine and model scale tests — conical nozzle at supersonic conditions.

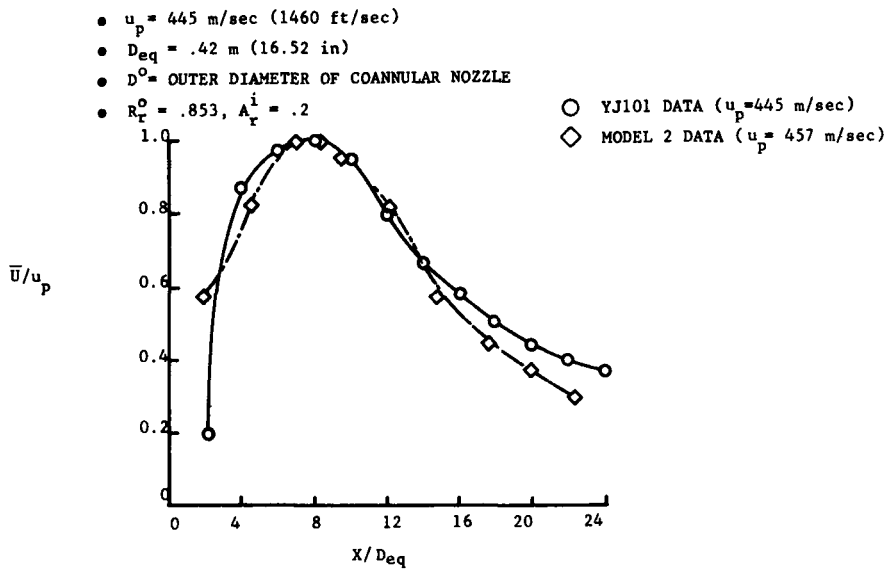

Figure 31.- Comparisons of laser velocimeter measured axial mean velocity decay for engine and model coannular plug nozzle tests — supersonic flow conditions.

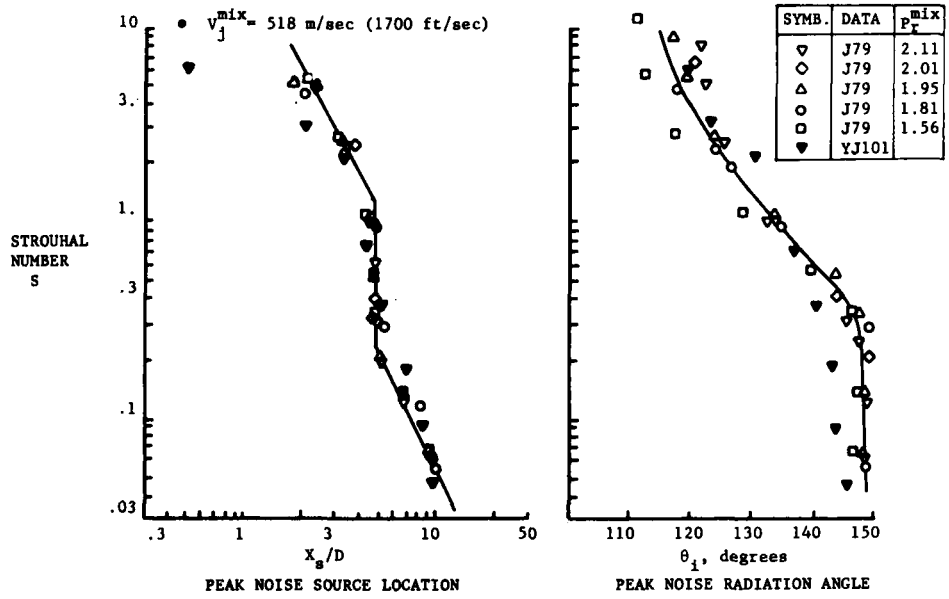

Figure 32.- Measured peak noise source locations and farfield radiation angles for J79 and YJ101/AST conic nozzles.

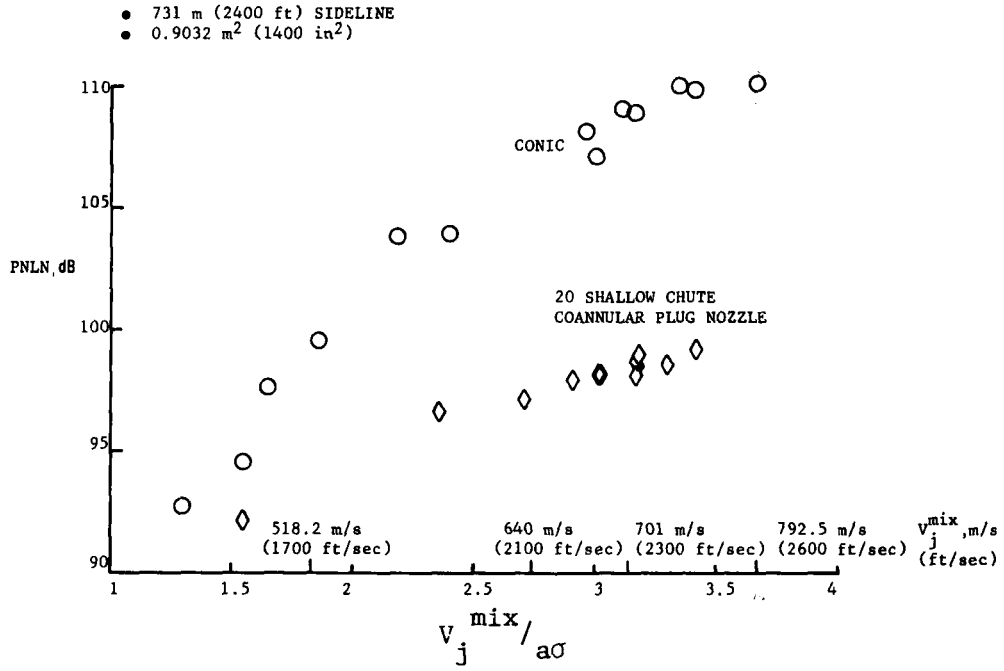

Figure 33.- Static jet noise reduction for a simple mechanical suppressor.

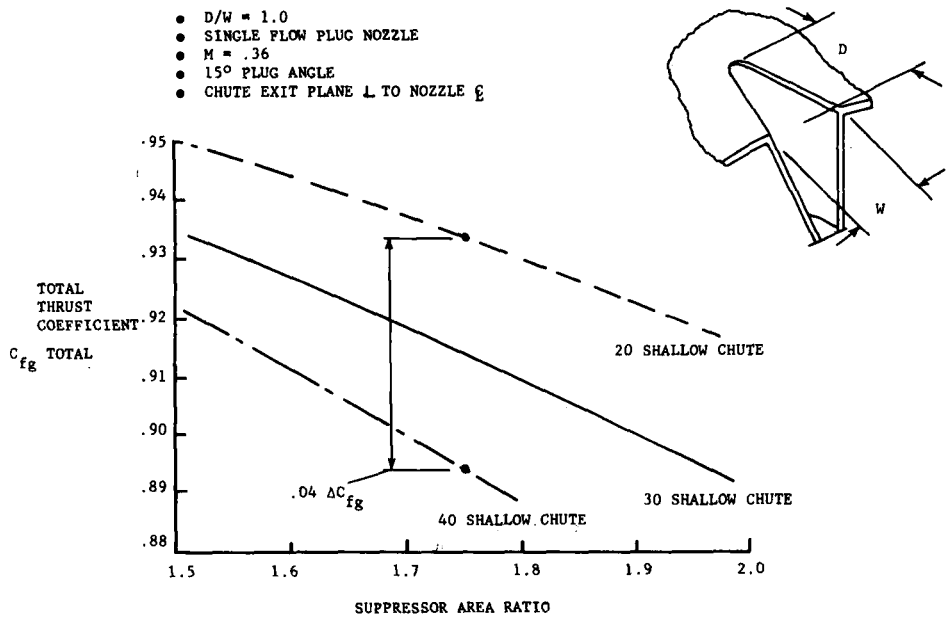

Figure 34.- Variation of total thrust coefficient with suppressor element number and area ratio.

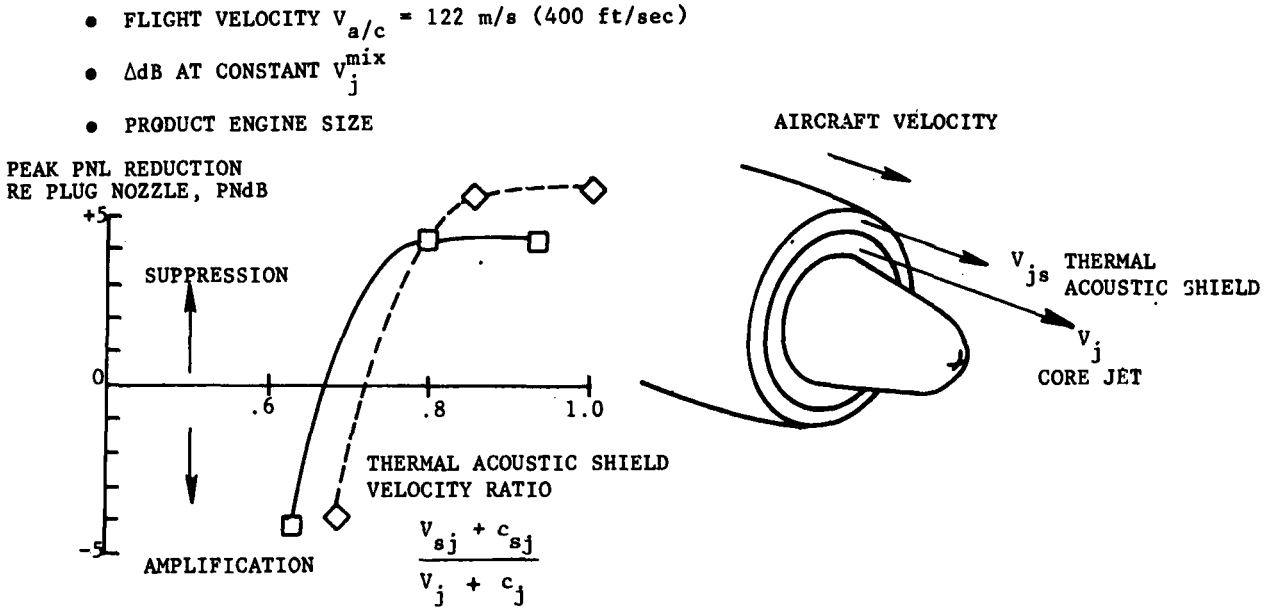

Figure 35.- Inflight thermal acoustic shield suppression.